DMD Fast Forward. Published on June 7, 2006 as doi:10.1124/dmd.106.010009

DMD #10009

Characterization of phenotypes in *Gstm1*-null mice by cytosolic and *in vivo* metabolic studies using DCNB

Kazunori Fujimoto, Shingo Arakawa, Yukari Shibaya, Hiroaki Miida, Yosuke Ando, Hiroaki Yasumo, Ayako Hara, Minoru Uchiyama, Haruo Iwabuchi, Wataru Takasaki, Sunao Manabe and Takashi Yamoto

Medicinal Safety Research Laboratories, Sankyo Co., Ltd., 717 Horikoshi, Fukuroi, Shizuoka 437-0065, Japan (KF, SA, YS, HM, YA, WT, SM, TY)

Biomedical Research Laboratories, Sankyo Co., Ltd., 1-2-58 Hiromachi, Shinagawa-ku, Tokyo 140-8710, Japan (HY, AH)

Drug Metabolism and Pharmacokinetics Research Laboratories, Sankyo Co., Ltd., 1-2-58 Hiromachi, Shinagawa-ku, Tokyo 140-8710, Japan (MU, HI)

DMD Fast Forward. Published on June 7, 2006 as DOI: 10.1124/dmd.106.010009
This article has not been copyedited and formatted. The final version may differ from this version.

Running title:

DCNB metabolism in *Gstm1*-null mice

Corresponding author:

Kazunori Fujimoto, Medicinal Safety Research Laboratories, Sankyo Co., Ltd., 717 Horikoshi, Fukuroi, Shizuoka 437-0065, Japan, Phone: +81-538-42-4356, Fax: +81-538-42-4350, E-mail: kazunf@sankyo.co.jp

Number of text pages: 24

Number of figures: 7

Number of tables: 0

Number of references: 22

Words in Abstract: 219 words

Words in Introduction: 316 words

Words in Discussion: 857 words

Abbreviations:

GST, glutathione *S*-transferase; DCNB, 1,2-dichloro-4-nitrobenzene; CDNB, 1-chloro-2,4-dinitrobenzene; GST-D activity, GST activity toward DCNB; GST-C activity, GST activity toward CDNB

DMD Fast Forward. Published on June 7, 2006 as DOI: 10.1124/dmd.106.010009
This article has not been copyedited and formatted. The final version may differ from this version.

Abstract

Glutathione S-transferase Mu 1 (GSTM1) has been regarded as one of the key enzymes involved in phase II reactions in the liver, due to its high expression level. In this study, we generated mice with disrupted glutathione *S*-transferase Mu 1 gene (*Gstm1*-null mice) by gene targeting, and characterized the phenotypes by cytosolic and *in vivo* studies. The resulting *Gstm1*-null mice appeared to be normal and were fertile. Expression analyses for the *Gstm1*-null mice revealed a deletion of *Gstm1* mRNA and a small decrease in *Gsta3* mRNA. In the enzymatic study, GST activities toward 1,2-dichloro-4-nitrobenzene (DCNB) and 1-chloro-2,4-dinitrobenzene (CDNB) in the liver and kidney cytosols were markedly lower in *Gstm1*-null mice than in the wild-type control. *Gstm1*-null mice had GST activities of only 6.1-21.0% of the wild-type control to DCNB and 26.0-78.6% of the wild-type control to CDNB. After a single oral administration of DCNB to *Gstm1*-null mice, the plasma concentration of DCNB showed larger $AUC_{0\text{-}24}$ (5.1-5.3 times, vs. the wild-type control) and higher C_{max} (2.1-2.2 times, vs. the wild-type control) with a correspondingly lower level of GSH-related metabolite ($AUC_{0\text{-}24}$: 9.4-17.9% and C_{max}: 9.7-15.6% of the wild-type control). In conclusion, *Gstm1*-null mice showed markedly low ability for glutathione conjugation to DCNB in the cytosol and *in vivo* and would be useful as a deficient model of GSTM1 for ADME/Tox studies.

Glutathione S-transferases (GSTs) form a superfamily that is characterized by catalysis of the conjugation of glutathione (GSH) with various electrophilic compounds (Hayes and Pulford, 1995). At least seven distinct classes (Alpha, Mu, Pi, Sigma, Theta, Kappa and Zeta) of soluble GSTs have been identified so far according to substrate specificity, chemical affinity, structure and the kinetic behavior of the enzyme (Landi, 2000; Strange et al., 2000). However, a large number of GST isoforms that overlap the substrates' specificities and broad GST expression in various tissues do not encourage the characterization of the properties for each GST isoform in the whole body.

The use of knockout mice with one disrupted gene among a large number of xenobiotic metabolizing enzyme isoforms shows great advantages in understanding the pharma/toxicokinetics of xenobiotics. Three knockout mice lines for GST isoforms, *Gsta4* KO mice (Engle et al., 2004), *Gstp1/p2* KO mice (Henderson et al., 1998; Henderson et al. 2000; Elsby et al. 2003) and *Gstz1* KO mice (Fernandez-Canon et al, 2002; Lim et al, 2004), have been established so far. However, the pharma/toxicokinetics of the specific substrate for the GST isoform in these knockout mice lines has not been analyzed yet. And there are only a few reports about the pharma/toxicokinetics of the specific substrate in the knockout mice with disrupted xenobiotic metabolizing enzyme genes other than GSTs.

In mouse, GSTA3, GSTP1 and GSTM1 show high expression levels in the liver and kidney, and have been regarded as the key enzymes for phase II reaction and the detoxification of carcinogens/mutagens, environmental pollutants and anticancer drugs (Mitchell et al., 1997). In this study, we focused on GSTM1, which is one of 6 Mu class GST isoforms in mice (Hayes and Pulford, 1995; Guo et al., 2002), and generated mice with disrupted glutathione *S*-transferase Mu 1 gene (*Gstm1*-null mice) by gene targeting. We characterized the phenotypes by *in vitro* and *in vivo*

metabolic studies.

DMD Fast Forward. Published on June 7, 2006 as DOI: 10.1124/dmd.106.010009
This article has not been copyedited and formatted. The final version may differ from this version.

Materials and methods

Generation of Gstm1-null mice

To construct the targeting vector, DNA from W9.5 ES cell was used to amplify *Gstm1* genomic fragments for both the 5' and 3' arms. For the 5' arm, a 6.8-kb 5'-flanking sequence of the *Gstm1* gene was cloned into the *Hpa*I and *Xho*I sites of the pKO Scrambler V901 plasmid. For the 3' arm, a 3.0-kb 3'-flanking sequence of the *Gstm1* gene was cloned into the *Sac*II and *Sal*I sites. The primers for the 5' arm were 5'-AGTGTTAACATGCTTTATTCATTCTTCCGACATC-3' and 5'-CCCCTCGAGAGTTACAGGAACAGTCGGTGACATG-3'. The primers for the 3' arm were 5'-AGACCGCGGGGTCTCTCCACCTTGCACATGCCAC-3' and 5'-CGCGTCGACACAGCATTCTCGTGAAAGATGTTTG-3'. For the positive negative selection, a Neomycin resistant (Neo^r) cassette from the pKO SelectNeo V800 plasmid and *Diphteria Toxin A chain* gene (DT) from pKO SelectDT V840 plasmid was used. All plasmids were supplied from TAKARA BIO Inc. (Ohtsu, Japan). W9.5 ES cells (10^7) were electroporated (250 V, 500 μF) with 20 μg of the linearized targeting vector and selected with 250 μg (active form)/ml G418 for 8-10 days (Fujimoto et al., 2006). G418 resistant clones were primarily screened on the 3' arm by PCR with the primer pair, NeoF3: 5'-CTGCTAAAGCGCATGCTCCAGACTGCCTTG-3' and M1R2: 5'-ACCTGTGAACTGGAGATCCAGAGCTCTTAC-3'. The PCR positive clones were twice checked on the 5' arm by PCR with the primer pair, GM2H: 5'-AGTGTTAACTTGTGAGGTTGACACAGAACTCTG-3' and NP3: 5'-AATGAGGAAATTGCATCGCATT-3'. Finally, the homologous recombination was confirmed by the direct sequence of the amplified PCR fragments on both regions using ABI PRISM 3700 DNA Analyzer (Applied Biosystems, Foster city, CA, U.S.A.). Chimera mice were generated using the

DMD Fast Forward. Published on June 7, 2006 as DOI: 10.1124/dmd.106.010009
This article has not been copyedited and formatted. The final version may differ from this version.

targeted ES cell clone by an aggregation method (Wood et al., 1993). Male chimera mice were mated with C57BL/6J females, and homozygous mutant (*Gstm1*-null) mice were obtained by intercrossing the heterozygotes. Their genotype was determined by PCR using two forward primers (NeoRF for the mutant allele: 5'-ACTTGTGTAGCGCCAAGTGCCCA-3', and GSTM1-WF for the wild allele: 5'-TCTCCTTGAGGAATGATGAGGCT-3') and one common reverse primer (GSTM1-WR: 5'-TTCTCCATGCCAGGAGAACTCTA-3'). Mice were housed under a controlled temperature (23±1°C) with free access to water and mouse chow. The experimental protocol was approved by the Ethics Review Committee for Animal Experimentation of Sankyo Co., Ltd.

Gstm1, Gsta3 and Gstp1 mRNA expression analysis

To analyze the *GST* isoform gene expression, total RNA was isolated from the livers of the *Gstm1*-null mice, the heterozygotes and the wild-type controls. After DNase I treatment, cDNA were synthesized using an oligo-dT primer and SuperScript II reverse transcriptase (Invitrogen, Carlsbad, CA, USA). RT-PCR was performed using the primers specific for the mouse *Gstm1* gene (forward: 5'-GCTCATCATGCTCTGTTACAAC-3', and reverse: 5'-TGTAGCAAGGGCCTACTTGT-3') and *beta-actin* gene (forward: 5'-ATGGAATCCTGTGGCATCCATG-3', and reverse: 5'-TAGAAGCACTTGCGGTGCACGAT-3'). Real time quantitative RT-PCR for the mouse *Gsta3*, *Gstp1* and *Gapdh* genes was performed using the TaqMan Gene Expression Assays (Applied Biosystems) and qPCR Mastermix Plus (Nippon EGT, Toyama, Japan). The mRNA content level was quantified with a GeneAmp 5700 Sequence Detection System (Applied Biosystems), according to the manufacturer's instruction.

Measurement of the GST activities toward CDNB and DCNB in the cytosols of the liver and kidney

The liver and kidney samples of the *Gstm1-null* mice, the heterozygotes and the wild-type controls were mixed with 1.15% potassium chloride (1/3, w/v) and homogenized in an ice bath. The homogenates were centrifuged at 9,000 × *g* for 20 minutes at 4°C, and the supernatant fraction was further centrifuged at 105,000 × *g* for 1 hour at 4°C to isolate the cytosolic fraction. Protein concentrations in the cytosolic fractions were determined by the method of Lowry *et al.* (1951). The GST activity toward CDNB (GST-C activity) was measured according to the established method (Habig et al, 1974). Briefly, the cytosol was diluted 30-fold with 1.15% potassium chloride, and 0.3 ml of 20 mM GSH and 0.06 ml of the diluted cytosol were mixed in 5.34 ml of 100 mM potassium phosphate buffer (pH 6.5). After the addition of CDNB at a final concentration of 1 mM, the change in absorbance at 340 nm was measured for 1 minute with a spectrophotometer. The GST activity toward DCNB (GST-D activity) was measured according to the established method (Habig, 1974). Briefly, the cytosol was diluted 30-fold with 1.15% potassium chloride, and 0.3 ml of 100 mM GSH and 0.1 ml of the cytosol were mixed with 5.3 ml of 100 mM potassium phosphate buffer (pH 7.5). After addition of DCNB at a final concentration of 1 mM, the change in absorbance at 345 nm was measured for 1 minute with a spectrophotometer. The GST-C and GST-D activities were expressed as the amount of CDNB-GSH and DCNB-GSH conjugate moles formed per unit weight of protein per unit of time, respectively.

Measurement of plasma DCNB and the metabolites concentrations after administration of DCNB

Gstm1-null mice and the wild-type controls were treated via oral administration with 1% DCNB

DMD Fast Forward. Published on June 7, 2006 as DOI: 10.1124/dmd.106.010009
This article has not been copyedited and formatted. The final version may differ from this version.

dissolved in polyethylene glycol at dose levels of 100 mg/kg. Approximately 0.3 ml of blood was collected at 30 min, 1, 2, 4, 8 and 24 h postdose. The blood samples were centrifuged at 10,000 rpm for 5 min at 4°C to prepare the plasma samples. Then, 50 μl of each plasma sample was mixed with 150 μl ethanol and centrifuged at 3,000 rpm for 5 min at 4°C. In order to determine the plasma concentration of DCNB, the supernatant was subjected to a high-performance liquid chromatograph (HPLC) system (Shimadzu corporation, Kyoto, Japan) consisting of a system controller (SCL-10A), a pump (LC-10AD), an autosampler (SIL-10A_{XL}), a column oven (CTO-10AC) and a UV detector (SPD-10A). The HPLC conditions for this analysis were as follows: the column was an L-column ODS (150×4.6 mm I.D., Chemicals Evaluation and Research Institute, Tokyo, Japan); the column temperature was 40°C; mobile phase water/Acetonitril/Ammonium acetate (1M) at 65/35/1 (v/v/v); flow rate 1.0 ml/min; injection volume 20 μl; and UV detector wavelength 270 nm.

LC-MS and LC-MS/MS Analyses

LC-MS and LC-MS/MS analyses were performed using a Q-Tof mass spectrometer (Waters, Manchester, UK) with an HPLC system (Hitachi High-Technologies Corp., Tokyo, Japan) consisting of an intelligent pump (model L-7100), a column oven (model L-7300), a chromato-integrator (model D-7500) and a UV detector (model L-7400S). The LC-MS analysis was conducted using electrospray ionization (ESI) in the positive ion mode. The capillary voltage and cone voltage were set at 3300 V and 45 V, respectively. The source temperature and desolvation gas temperature were 120°C and 300°C, respectively. The mass range from *m/z* 50 to 900 was acquired with an integration time of 1 sec. The LC-MS/MS experiments were performed using a collision energy of 20 eV and xenon as the collision gas. The chromatographic separation was carried out on a YMC-Pack ODS-A A-312 column (6.0 × 150 mm, YMC Corporation, Kyoto, Japan), the column temperature was

maintained at 40°C and UV detection was at 270 nm. The mobile phase used was a water/acetonitrile/ammonium acetate (1 M) at a ratio of 82/18/1 (v/v/v). The flow rate was set at 0.1 ml/min and the elution flow from HPLC was introduced into the Q-Tof ionization source through an ESI interface.

Statistical analysis

The values of the mean and the standard deviation in each group were calculated with statistical software (SAS System Version 5.0: SAS Institute Inc., Cary, NC, USA). A parametric Dunnett's test for the mean value was performed to analyze the differences between the wild-type control and the hetero/homozygote. A value of $P < 0.05$ was chosen as an indication of statistical significance.

DMD Fast Forward. Published on June 7, 2006 as DOI: 10.1124/dmd.106.010009
This article has not been copyedited and formatted. The final version may differ from this version.

Results

Generation of Gstm1-null mice

Mice with disrupted *Gstm1* gene were generated by a homologous recombination method with a mouse ES cell. The targeting vector used in this study is shown in Figure 1A. Mouse *Gstm1* gene consists of 8 exons in a region of about 5.7 kb. This targeting vector was designed to achieve the deletion of the entire coding region of the *Gstm1* gene by replacing it with a Neo^r cassette. W9.5 ES cells were electroporated with the targeting vector and 288 of the colonies with G418 resistance were selected and screened by PCR for homologous recombination. Two independent PCR-positive clones, 4B3 and 10C4, were obtained by primary PCR screening with a NeoF3/M1R2 primer pair (Figure 1B, right). However, secondary PCR screening with a GM2H/NP3 primer pair revealed that only the 4B3 clone was integrated into the targeted sequence by homologous recombination (Figure 1B left). The 4B3 ES cells were aggregated with two zona-pellucida free 8-cell embryos from C57BL/6J mice, and cultured for 24 h. Aggregated blastcysts were transferred into the uteros of the surrogate mothers. Chimera mice were identified by coat color and crossed to C57BL/6J mice, and F1 heterozygous offspring to which the targeted ES cells had contributed were identified by coat color and PCR genotyping. Furthermore, the F_1 heterozygous mice were intercrossed to produce F_2 mice, which were determined to be wild-type (+/+), heterozygotes (+/-) or homozygotes (-/-; *Gstm1*-null mice) by PCR genotyping (Figure 2A). *Gstm1*-null mice appeared to be normal and were fertile as the wild-type and heterozygote. No obvious histological, hematological and blood chemical differences in the basal condition were detected between *Gstm1*-null mice and the wild-type control (data not shown).

DMD Fast Forward. Published on June 7, 2006 as DOI: 10.1124/dmd.106.010009
This article has not been copyedited and formatted. The final version may differ from this version.

Gstm1, Gsta3 and Gstp1 mRNA expression analysis

Gstm1 mRNA expression was not detected in the livers of *Gstm1*-null mice by RT-PCR (Figure 2B). This result indicates a disruption of the *Gstm1* gene in *Gstm1*-null mice. Furthermore, to confirm whether *Gstm1* gene disruption has an effect on *Gsta3* and *Gstp1* mRNA expression, the expression levels in the livers of *Gstm1*-null mice were determined by real time quantitative RT-PCR. These results revealed slightly low *Gsta3* mRNA expression levels (male; 64.7%, female; 86.5% of the wild-type control), despite the same levels of *Gstp1* mRNA expression in the livers of *Gstm1*-null mice (Figure 3).

GST-C and GST-D activity in the cytosol of the liver and kidney

We measured the GST-C and GST-D activity in cytosolic samples from the livers and kidneys of *Gstm1*-null mice. The results revealed low GST-C and GST-D activity in the *Gstm1*-null mice (Figure 4). GST-C activity was slightly low in the liver of the males (78.6% of the wild-type control), and markedly low in the liver of females (32.3% of the wild-type control) and in the kidneys of both sexes (male; 26.0%, female; 33.8% of the wild-type control). GST-D activity was nearly absent in the livers and the kidneys of both sexes (male liver; 9.9%, female liver; 8.7%, male kidney; 6.1%, female kidney; 21.0% of the wild-type control). The heterozygotes showed intermediate GST-C and GST-D activity between that of the homozygotes and wild-types in the all cytosolic samples.

Plasma concentrations of DCNB and its metabolite, M0, after administration of DCNB

We measured the plasma concentrations of DCNB after a single oral administration of DCNB (100 mg/kg) to wild-type and *Gstm1*-null mice by HPLC, in order to evaluate the pharmacokinetics of DCNB in the whole body. This result is shown in Figure 5. The $AUC_{0\text{-}24}$ was 6.04±0.62 μg·h/ml in the male wild-type control, 31.72±9.44 μg·h/ml in the male *Gstm1*-null mice, 9.02±1.27 μg·h/ml in

DMD Fast Forward. Published on June 7, 2006 as DOI: 10.1124/dmd.106.010009
This article has not been copyedited and formatted. The final version may differ from this version.

the female wild-type control and 45.99±5.34 μg·h/ml in the female *Gstm1*-null mice. The C_{max} was 1.76±0.53 μg/ml in the male wild-type control, 3.73±0.62 μg/ml in the male *Gstm1*-null mice, 1.95±0.23 μg/ml in the female wild-type control and 4.30±0.22 μg/ml in the female *Gstm1*-null mice. After a single oral administration of DCNB to *Gstm1*-null mice, the plasma concentration of DCNB showed a larger $AUC_{0\text{-}24}$ (male; 5.3 times, female; 5.1 times, vs. the wild-type control) and higher C_{max} (male; 2.1 times, female; 2.2 times, vs. the wild-type control). Furthermore, three peaks were determined in the plasma after administration of DCNB to the wild-type control, as major metabolite peaks in HPLC chromatogram. As shown in Figure 6, the concentration of M0, which had the highest level among the three metabolites, was lower in the plasma of *Gstm1*-null mice. After a single oral administration of DCNB to *Gstm1*-null mice showed smaller $AUC_{0\text{-}24}$ (male; 9.4%, female; 17.9% of the wild-type control) and lower C_{max} (male; 9.7%, female; 15.6% of the wild-type control).

Structure Analysis of Metabolite M0

The DCNB metabolite, M0, was detectable in a mouse plasma. The molecular-related ion $[M+H]^+$ of M0 was observed at *m/z* 248 in the positive ion mode. Thus, the molecular weight of metabolite M0 was proposed to be 247. The LC-MS/MS spectrum of the precursor ion $[M+H]^+$ at *m/z* 248 and major fragment ions are shown in Figure 7. The fragment ion at *m/z* 206 was formed via elimination of the acetyl moiety from the ion at *m/z* 248. The fragment ion at *m/z* 170 was formed via elimination of the methylsulfon moiety from the ion at *m/z* 248. In addition, the most intense fragment ion at *m/z* 127 was formed by loss of the acetyl moiety and the methylsulfon moiety from the ion at *m/z* 248. As well, a high resolution LC-ESI/MS analysis demonstrated the elemental composition of the molecular-related ion $[M+H]^+$ at *m/z* 248 to be $C_9H_{11}NO_3SCl$ (data not shown),

DMD Fast Forward. Published on June 7, 2006 as DOI: 10.1124/dmd.106.010009
This article has not been copyedited and formatted. The final version may differ from this version.

which supports the fact that metabolite M0 is a methylsulfon-*N*-acetyl form of DCNB. Therefore, the chemical structure of M0 was found to be a methylsulfon-*N*-acethyl form produced by the glutathion conjugation of the DCNB followed by several metabolic reactions.

Discussion

We generated mice with disrupted *Gstm1* gene, which is expressed predominantly in the liver, by homologous recombination, in order to investigate the properties of mouse GSTM1 in xenobiotic metabolism. An ES cell clone with the predicted mutant allele, confirmed by genomic PCR and sequencing analyses, was used to generate mice with disrupted *Gstm1* gene. RT-PCR analysis revealed a lack of *Gstm1* mRNA expression in the homozygote. Furthermore, two-dimensional difference gel electrophoresis/mass spectrometry analyses also revealed that GSTM1 protein expression was completely absent in the homozygotes (data not shown). These results indicated success in the generation of the *Gstm1*-null mice.

In the enzymatic study, GST-D activity was nearly absent in the livers and kidneys of both sexes in *Gstm1*-null mice. Mouse GSTM1 purified from liver cytosol has been reported to specifically catalyze DCNB (Warholm et al., 1986). The present study also clarified that DCNB is a specific substrate for mouse GSTM1. On the other hand, *Gstm1*-null mice showed low GST-C activity (approximately 30% of the wild-type control) in the kidneys of both sexes and in the female livers, and a slightly low GST-C activity (approximately 80% of the wild-type control) in the male livers. Interestingly, GST-C activities with broad specificity to various GSTs were lower than our expectation in the male and female kidneys and the female livers of the *Gstm1*-null mice, indicating that GSTM1 is the main enzyme to catalyze CDNB metabolism in mouse male and female kidneys and female livers. The higher hepatic GST-C activity in the male *Gstm1*-null mice may be owing to the higher expression of Pi class GSTs in males than females (Mitchell et al., 1997).

Plasma DCNB concentrations after an administration of DCNB to *Gstm1*-null mice showed larger $AUC_{0\text{-}24}$ (male; 5.3 times, female; 5.1 times, vs. the wild-type control) and higher C_{max} (male; 2.1

DMD Fast Forward. Published on June 7, 2006 as DOI: 10.1124/dmd.106.010009
This article has not been copyedited and formatted. The final version may differ from this version.

times, female; 2.2 times, vs. the wild-type control), consistently with lower GST-D activity *in vitro*. Correspondingly, the concentration of M0, the major metabolite among the three DCNB metabolites separated on HPLC chromatogram, showed smaller $AUC_{0\text{-}24}$ in the plasma (male; 9.4%, female; 17.9% of the wild-type control) and lower C_{max} (male; 9.7%, female; 15.6% of the wild-type control) in *Gstm1*-null mice. This suggested that M0 might be a GSH-related metabolite of DCNB. Actually, the structure analysis by LC-MS/MS revealed that M0 was the GSH-related metabolite, the methylsulfon-*N*-acetyl form (Bray et al., 1957; Bray et al., 1957; Zhang et al., 2003). Considering these results, *Gstm1*-null mice administered the specific substrate for mouse GSTM1, such as DCNB, are highly exposed and toxicologically susceptible to the substrate. Therefore, we conclude that *Gstm1*-null mice would be useful as a toxicokinetically modified animal model, i.e. an animal model of a poor metabolizer to the specific substrates for mouse GSTM1.

We performed comprehensive gene expression analysis of the livers of the *Gstm1*-mice and the wild-type controls using Affymetrix GeneChip microarray. This result showed that no GST isoforms were upregulated in *Gstm1*-null mice (data not shown), different from the case of *Gsta4*-null mice and *Gstz1*-null mice (Engle et al., 2004; Lim et al, 2004). In *Gstm1*-null mice, slightly low expression level of *Gsta3* mRNA was observed by GeneChip microarray and real time quantitative RT-PCR analyses, despite there being no change in the *Gstp1* mRNA expression level. It has been actually reported that mouse GSTA3 has low GST-C and GST-D activities (Hayes and Pulford, 1995). From these results and available information, the slight down-regulation of the *Gsta3* mRNA expression might be involved in low GST-C and GST-D activities in *Gstm1*-null mice established in this study.

GSTs are important enzymes for xenobiotic metabolism and toxic phenotype. However, a large

number of GST isoforms overlap the substrates' specificities and a broad GST expression in various tissues could not facilitate the characterization of the properties of each GST isoform in the whole body. The GST knockout mice would facilitate the investigation of these properties and help to understand the metabolic pathways through the GST isoforms (Hayes et al., 2005). However, only a few reports on GST knockout mice have been published so far. In the present study, we generated knockout mice for the *Gstm1* gene, and clarified that the GSTM1 deficiency results in markedly low GST-D activity both *in vitro* and *in vivo*. Furthermore, it has been reported that mouse GSTM1 inhibits apoptosis signal-regulating kinase 1 (ASK1) by forming GSTM1/ASK1 complex and mediates apoptosis in response to heat shock stress (Cho et al., 2001; Dorion et al., 2002). These observations suggest that GSTM1 is responsible not only as a xenobiotic metabolizing enzyme but also as cellular signaling factor. *Gstm1*-null mice would be useful to analyze the apoptosis signaling via GSTM1 *in vivo*.

In conclusion, we generated knockout mice for the *Gstm1* gene, and found that GST-D activity in the liver and kidney cytosols markedly decreased in *Gstm1*-null mice, and that a single oral administration of DCNB to *Gstm1*-null mice resulted in larger AUC and higher C_{max} for the plasma concentration of DCNB, and smaller AUC and lower C_{max} for the plasma concentration of M0, GSH-related metabolite of DCNB. This mouse would be useful as an animal model exhibiting poor metabolism of the specific substrates to mouse GSTM1 for ADME/TOX study.

DMD Fast Forward. Published on June 7, 2006 as DOI: 10.1124/dmd.106.010009
This article has not been copyedited and formatted. The final version may differ from this version.

Acknowledgements

We would like to thank T. Matsuura, Y. Aida, S. Yamauchi, K. Watanabe and M. Kiyosawa for their excellent technical assistance.

References

Bray HG, James SP and Thorpe WV (1957) The metabolism of 2:4-, 2:5- and 3:4-dichloronitrobenzene in the rabbit. *Biochem J* **65**:483-490.

Bray HG, James SP and Thorpe WV (1957) The metabolism of 2:3-, 2:6- and 3:5-dichloronitrobenzene in the rabbit. *Biochem J* **67**:607-616.

Cho SG, Lee YH, Park HS, Ryoo K, Kang KW, Park J, Eom SJ, Kim MJ, Chang TS, Choi SY, Shim J, Kim Y, Dong MS, Lee MJ, Kim SG, Ichijo H, Choi EJ (2001) Glutathione *S*-Transferase Mu Modulates the Stress-activated Signals by Suppressing Apoptosis Signal-regulating Kinase 1. *J Biol Chem* **276**:12749-12755.

Dorion S, Lambert H and Landry J (2002) Activation of the p38 signaling pathway by heat shock involves the dissociation of glutathione S-transferase Mu from Ask1. *J Biol Chem* **277**:30792-30797.

Elsby R, Kiiteringham NR, Goldring CE, Lovatt CA, Chamberlain M, Henderson CJ, Wolf CR, Park BK (2003) Increased constitutive c-Jun N-terminal kinase signaling in mice lacking glutathione S-transferase Pi. *J Biol Chem* **278**:22243-22249.

Engle MR, Singh SP, Czernik PJ, Gaddy D, Montague DC, Ceci JD, Yang Y, Awasthi S, Awasthi YC and Zimniak P (2004) Physiological role of mGSTA4-4, a glutathione S-transferase metabolizing 4-hydroxynonenal: generation and analysis of *mGsta4* null mouse. *Toxicol Appl Pharmco* **194**:296-308.

Fernandez-Canon JM, Baetscher MW, Finegold M, Burlingame T, Gibson KM and Grompe M (2002) Maleylacetoacetate isomerase (MAAI/GSTZ)-deficient mice reveal a glutathione-dependent nonenzymatic bypass in tyrosine catabolism. *Mol Cell Biol*

22:4943-4951.

Fujimoto K, Koishi R, Shimizugawa T and Ando Y (2006) Angptl3-null mice show low plasma lipid concentrations by enhanced lipoprotein lipase activity. *Exp Anim* **55**:27-34.

Guo J, Zimniak L, Zimniak P, Orchard JL and Singh SV (2002) Cloning and expression of a novel Mu class murine glutathione transferase isoenzyme. *Biochem J* **366**:817-824.

Habig WH, Pabst MJ and Jakoby WB (1974) Glutathione S-transferases. The first enzymatic step in mercapuric acid formation. *J Biol Chem* **249**:7130-7139.

Hayes JD, Flanagan JU and Jowsey IR (2005) Glutathione transferases. *Annu Rev Pharmacol Toxicol* **45**:51-88.

Hayes JD and Pulford DJ (1995) The glutathione S-transferase supergene family: Regulation of GST and the contribution of the isoenzymes to cancer chemoprotection and drug resistance. *Crit Rev Biochem Mol Biol* **30**:445-600.

Henderson CJ, Smith AG, Ure J, Brown K, Bacon EJ and Wolf CR (1998) Increased skin tumorigenesis in mice lacking pi class glutathione S-transferases. *Proc Natl Acad Sci USA* **95**:5275-5280.

Henderson CJ, Wolf CR, Kitteringham N, Powell H, Otto D, Park BK (2000) Increased resistance to acetaminophen hepatotoxicity in mice lacking glutathione S-transferase Pi. *Proc Natl Acad Sci USA* **97**:12741-5.

Landi S (2000) Mammalian class theta GST and differential susceptibility to carcinogens: a review. *Mutat Res* **463**:247-283.

Lim CE, Matthaei K, Blackbum AC, Davis RP, Dahlstrom JE, Koina ME, Anders MW and Board PG (2004) Mice deficient in glutathione transferase zeta/maleylacetoacetate isomerase

exhibit a range of pathological changes and elevated expression of alpha, mu, and pi class glutathione transferases. *Am J Pathol* **165**:679-693.

Lowry OH, Rosebrough HJ, Farr AL and Randall RJ (1951) Protein measurement with the folin phenol reagent. *J Biol Chem* **193**:265-275.

Mitchell AE, Morin D, Lakritz J and Jones AD (1997) Quantitative profiling of tissue- and gender-related expression of glutathione S-transferase isoenzymes in the mouse. *Biochem J* **325**:207-216.

Strange RC, Jones PW and Fryer AA (2000) Glutathione S-transferase: genetics and role in toxicology. *Toxicol Lett* **112-113**:357-363.

Warholm M, Jensson H, Tahir MK, Mannervik B (1986) Purification and characterization of three distinct glutathione transferase from mouse liver. *Biochemistry* **25**:4119-4125.

Wood SA, Allen ND, Rossant J, Auerbach A and Nagy A (1993) Non-injection methods for the production of embryonic stem cell-embryo chimaeras. *Nature* **365**:87-89.

Zhang JY, Yuan JJ, Wang YF, Bible RH Jr and Breau AP (2003) Pharmacokinetics and metabolism of a COX-2 inhibitor, valdecoxib, in mice. *Drug Metab Dispos* **31**:491-501.

Footnotes

Reprint requests: Kazunori Fujimoto, Medicinal Safety Research Laboratories, Sankyo Co., Ltd., 717 Horikoshi, Fukuroi, Shizuoka 437-0065, Japan. Phone: +81-538-42-4356, Fax: +81-538-42-4350, E-mail: kazunf@sankyo.co.jp

Legends for Figures

Figure 1. Targeted disruption of the mouse *Gstm1* gene. (A) The targeting vector construct (top), the wild allele of the *Gstm1* gene (middle) and the predicted mutant allele (bottom). The targeting vector was constructed by replacing the entire *Gstm1* gene contained 8 exons with Neomycin resistant (Neo^r) cassette. The *Diphteria toxin A chain* gene (DT) fragment was ligated at the 5' end of the vector for negative selection. The mutant allele was detectable by PCR using the indicated primer sets, GM2H/NP3 and NeoF3/M1R2, which confirmed the homologous recombination on the 5' and 3'arm, respectively. (B) PCR analyses of the homologous recombination on the 5' and 3' arm. GM2H/NP3 primer set was amplified a 7.15-kb fragment contained the 5' arm on the mutant allele (left). NeoF3/M1R2 primer set was amplified a 3.1-kb fragment contained the 3' arm on the mutant allele (right). Lambda/HindIII digest was used as a molecular size marker.

Figure 2. PCR genotyping and RT-PCR analysis of *Gstm1*-null mice. +/+, +/- and -/- indicated wild-type, heterozygote and homozygote, respectively. (A) The genotype was determined by PCR using two forward primers distinctive between the wild allele and the mutant allele and one common reverse primer. The wild allele and the mutant allele indicated a 154-bp fragment and a 236-fragment, respectively. Phi X174/HincII digest was used as a molecular size marker. (B) RT-PCR was performed using the primers specific for the mouse *Gstm1* gene and *beta-actin* gene. The amplified fragments were confirmed by the direct sequence using ABI PRISM 3700 DNA Analyzer.

Figure 3. Quantification of *Gsta3* and *Gstp1* mRNA in the liver of *Gstm1*-null mice. Messenger RNA from the livers of each five mice were qualified by the TaqMan Gene Expression Assays

(Applied Biosystems) using *Gapdh* mRNA as an internal control. The open and filled bars indicate wild-type and *Gstm1*-null mice, respectively. The values are depicted as the mean ± S.D. of five mice per group. The significant differences to the wild-type are shown as * $P < 0.01$.

Figure 4. GST-C and GST-D activity in cytosolic sample of the liver and kidney. Enzymatic activity was measured spectrophotometrically. Open, gray and filled bars indicate wild-type, heterozygote and homozygote, respectively. The values are depicted as the mean ± S.D. of five mice per group. The significant differences to the wild-type are shown as * $P < 0.05$, ** $P < 0.005$, *** $P < 0.001$.

Figure 5. Plasma DCNB concentrations after a single-dose oral administration of DCNB (100 mg/kg) to *Gstm1*-null mice or the wild-type control. Open and filled squares indicate wild-type control and *Gstm1*-null mice, respectively. The values are depicted as the mean ± S.E.M. of three mice per group.

Figure 6. Plasma M0 concentrations after a single-dose oral administration of DCNB (100 mg/kg) to *Gstm1*-null mice or the wild-type control. Open and filled squares indicate wild-type control and *Gstm1*-null mice, respectively. The values are depicted as mean ± S.E.M. of three mice per group.

Figure 7. MS/MS spectrum of metabolite M0 and proposed assignments of the fragment ions.

DMD Fast Forward. Published on June 7, 2006 as DOI: 10.1124/dmd.106.010009
This article has not been copyedited and formatted. The final version may differ from this version.

Figure 1

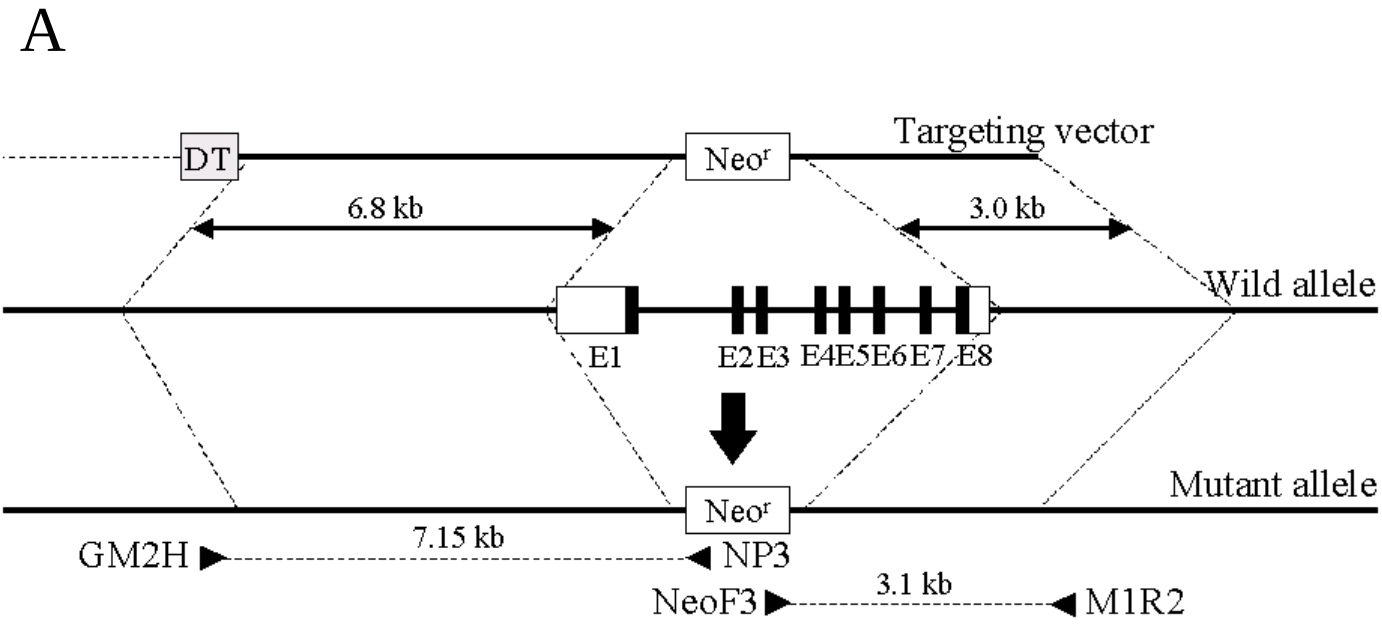

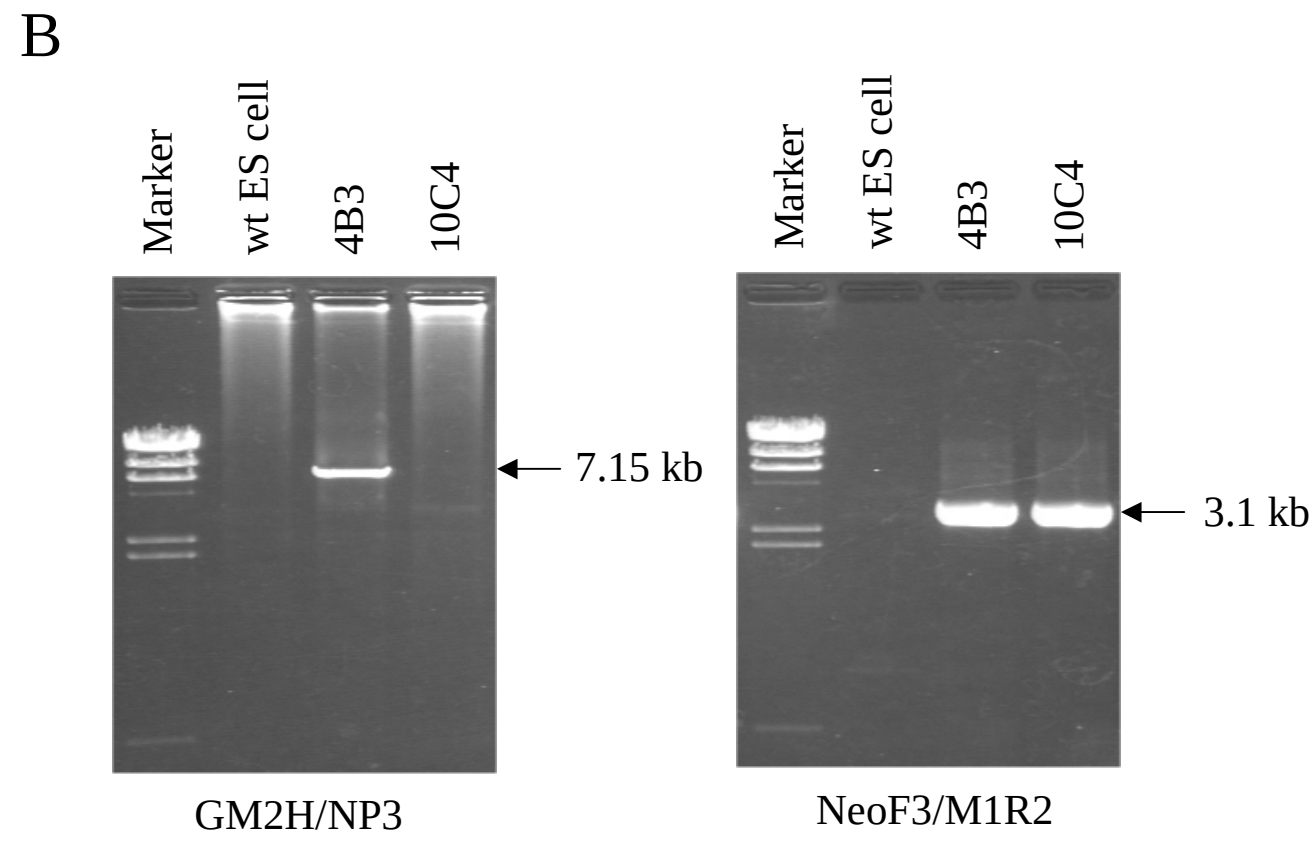

DMD Fast Forward. Published on June 7, 2006 as DOI: 10.1124/dmd.106.010009
This article has not been copyedited and formatted. The final version may differ from this version.

Figure 2

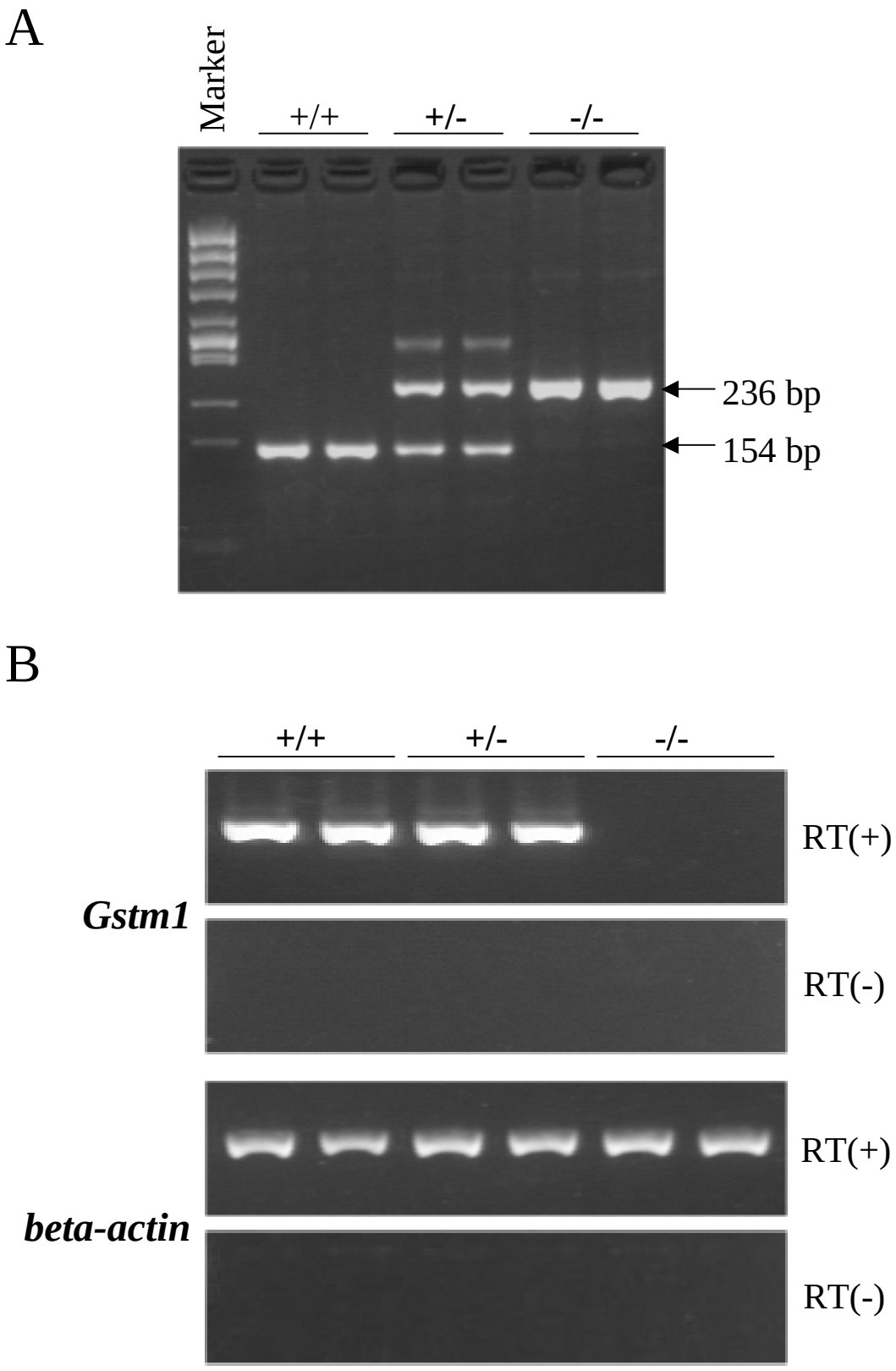

DMD Fast Forward. Published on June 7, 2006 as DOI: 10.1124/dmd.106.010009
This article has not been copyedited and formatted. The final version may differ from this version.

Figure 3

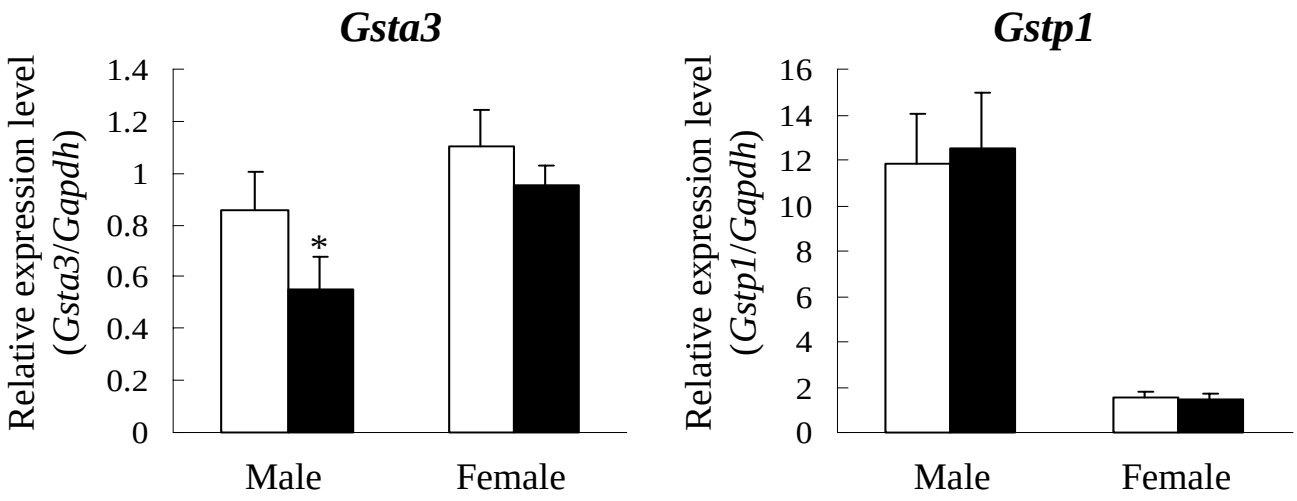

DMD Fast Forward. Published on June 7, 2006 as DOI: 10.1124/dmd.106.010009
This article has not been copyedited and formatted. The final version may differ from this version.

Figure 4

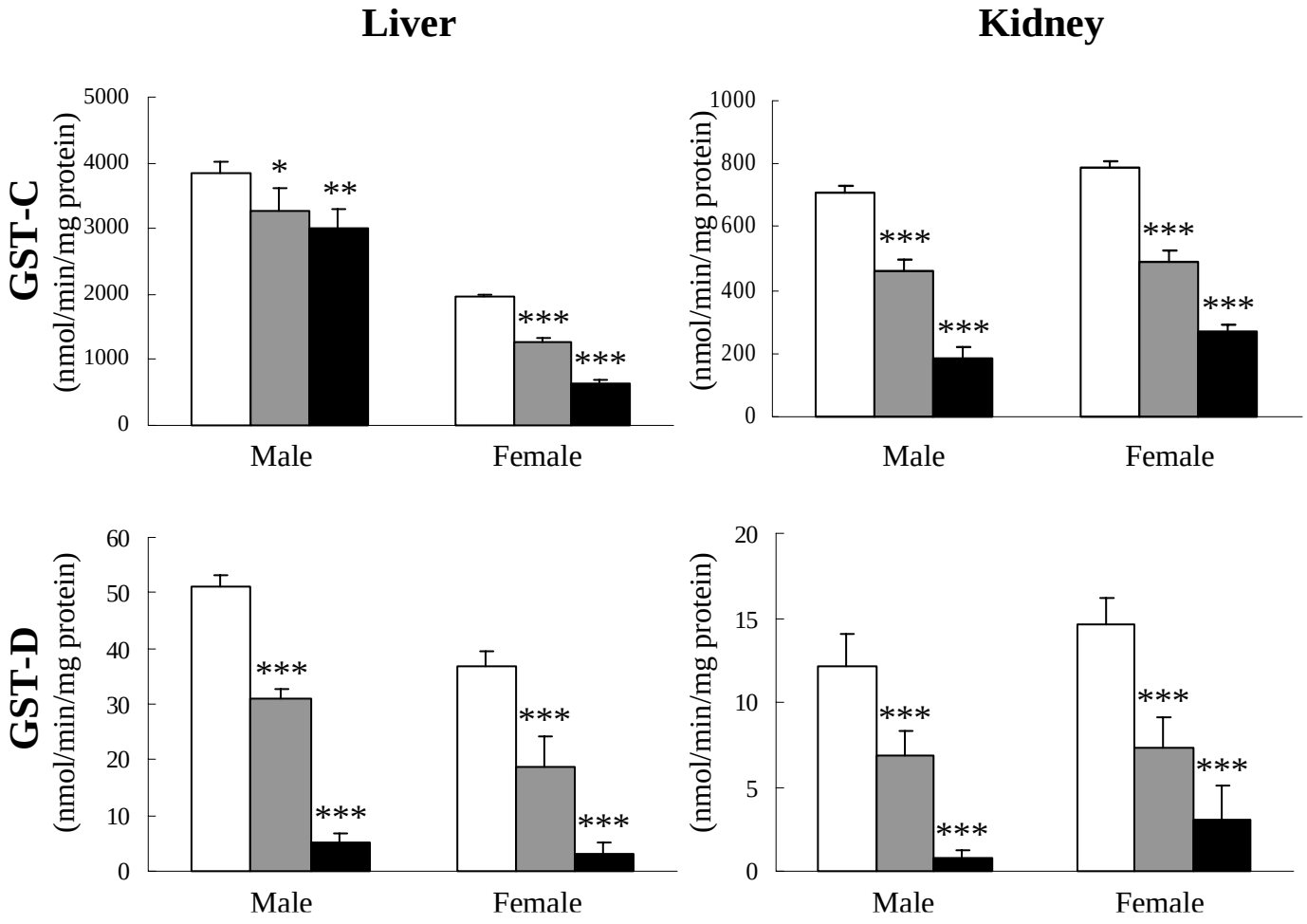

DMD Fast Forward. Published on June 7, 2006 as DOI: 10.1124/dmd.106.010009

Figure 5

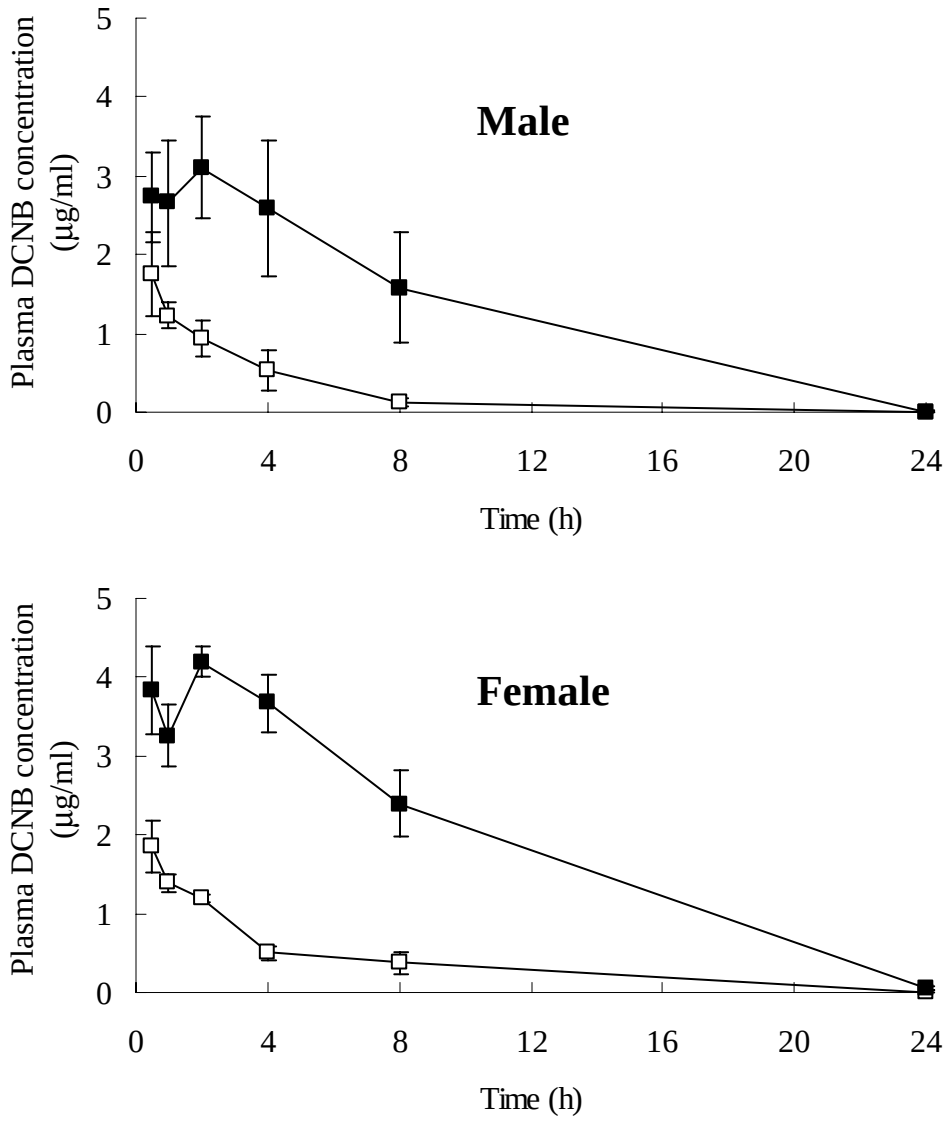

DMD Fast Forward. Published on June 7, 2006 as DOI: 10.1124/dmd.106.010009
This article has not been copyedited and formatted. The final version may differ from this version.

Figure 6

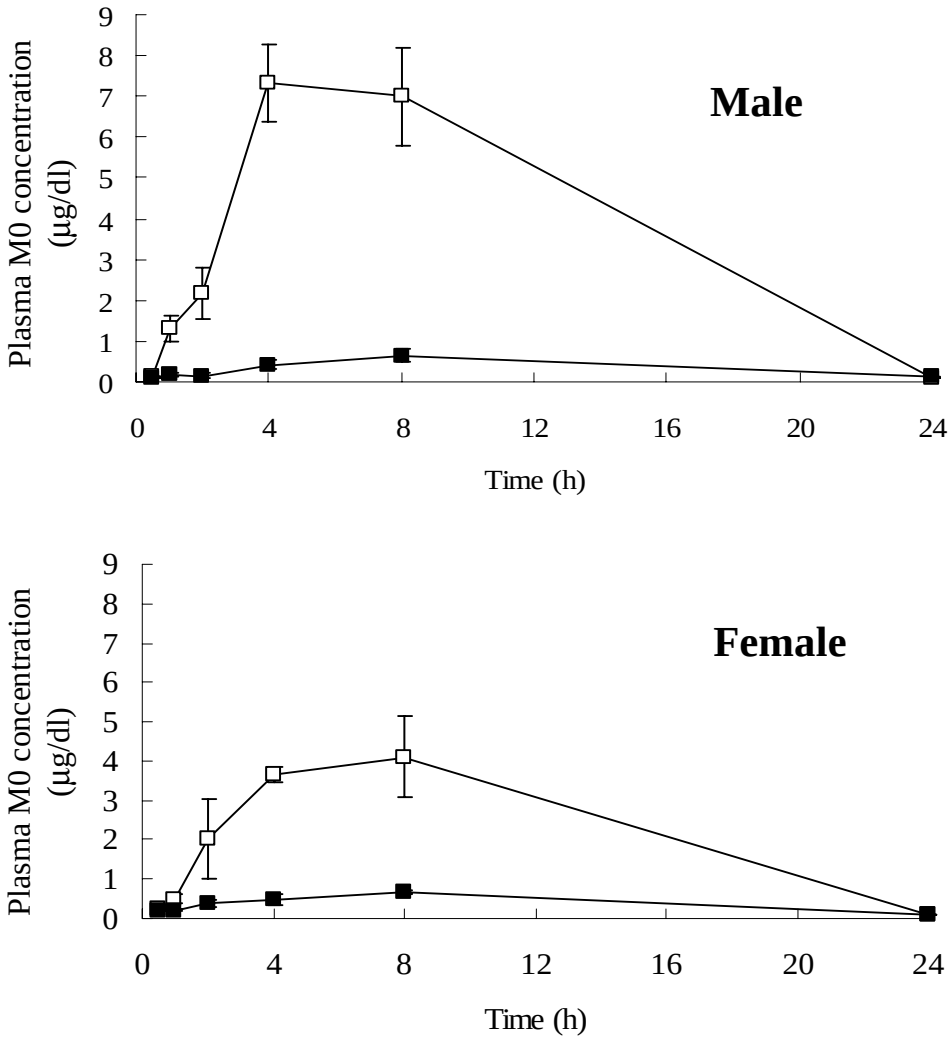

Figure 7